

An Efficient Adaptive Procedure for Three-Dimensional Fragmentation Simulations*

A. Pandolfi¹ and M. Ortiz²

¹Structural Engineering Department, Politecnico di Milano, Milano, Italy; ²Graduate Aeronautical Laboratories, California Institute of Technology, Pasadena, CA, USA

Abstract. *We present a simple set of data structures, and a collection of methods for constructing and updating the structures, designed to support the use of cohesive elements in simulations of fracture and fragmentation. Initially, all interior faces in the triangulation are perfectly coherent, i.e. conforming in the usual finite element sense. Cohesive elements are inserted adaptively at interior faces when the effective traction acting on those faces reaches the cohesive strength of the material. The insertion of cohesive elements changes the geometry of the boundary and, frequently, the topology of the model as well. The data structures and methods presented here are straightforward to implement, and enable the efficient tracking of complex fracture and fragmentation processes. The efficiency and versatility of the approach is demonstrated with the aid of two examples of application to dynamic fracture.*

Keywords. 3D finite elements; Adaptive remeshing; Cohesive elements; Fracture; Fragmentation; Topological changes

1. Introduction

The essential interplay between geometry and mechanics comes into sharp focus in applications where the topology of the domain may change, often extensively, during the course of calculations. Fragmentation, which may result in a runaway proliferation of bodies in the form of fragments [1–4], provides a case in point.

Camacho and Ortiz [5,6] in two dimensions, and Pandolfi *et al.* [7–9] in three dimensions, have established the feasibility of: (i) accounting explicitly for

individual cracks as they nucleate, propagate, branch and possibly link up to form fragments; and (ii) simulating explicitly the granular flow which ensues following widespread fragmentation. In this approach, cracks are allowed to form and propagate along element boundaries in accordance with a cohesive-law model [10,11]. Clearly, it is incumbent upon the mesh to provide a rich enough set of possible fracture paths, an issue which may be addressed within the framework of adaptive meshing. In contrast to other approaches [10,11], which require interfacial elements to be inserted at the outset along potential fracture paths, Camacho and Ortiz [5] and Pandolfi *et al.* [7–9] adaptively create a new surface as required by the cohesive model by duplicating nodes along previously coherent element boundaries, and inserting surface-like *cohesive elements* which encapsulate the fracture behavior of the solid. These elements are surface-like, and are compatible with general bulk finite element discretizations of the solid, including those which account for plasticity and large deformations.

Pandolfi and Ortiz [12] have given an enumeration of the ways in which the topology and geometry of a three-dimensional finite-element model may evolve as a consequence of fracture and fragmentation, and have described the actions which may be taken to update the boundary representation (or *Brep*) of the solid. Maintaining an up-to-date Brep is of the essence when meshing methods such as the advancing front [13–15] are utilized [16]. The Brep may also assist in the implementation of contact algorithms [17]. The geometrical framework proposed by Pandolfi and Ortiz [12] has been utilized extensively in a broad range of applications involving fracture and fragmentation [7–9].

The Brep of a solid can become inordinately complex, and thus computationally costly to maintain, in applications involving profuse fragmentation.

Correspondence and offprint requests to: Professor M. Ortiz, Graduate Aeronautical Laboratories, California Institute of Technology, 115 Firestone, Mailstop 105-50, Pasadena, CA 91125, USA. E-mail: ortiz@aero.caltech.edu

* Dedicated to Professor Giulio Maier on the occasion of his anniversary.

In addition, some meshing algorithms (e.g. those based on subdivision [18]) and contact algorithms (e.g. [19]) do not require a full Brep for their implementation. In these cases, much simpler data structures suffice to account for fragmentation processes.

The purpose of this paper is to present one such set of data structures, and a suite of methods for constructing and updating the structures. The data structures and methods are straightforward to implement, and enable the efficient tracking of complex fracture and fragmentation processes. We also present two examples of the application to dynamic fracture, which illustrate the ability of the method to represent intricate geometrical and topological transitions resulting from crack branching, the nucleation of surfaces and interior cracks, crack coalescence, the detachment of fragments, and other effects.

The organization of the paper is as follows. In Section 2 we introduce three simple data structures where all necessary information pertaining to tetrahedra, faces and edges is stored. In Section 3 we present the suite of methods for evolving the data structures in response to fragmentation. Finally, in Section 4 we present examples of application which demonstrate the scope and versatility of the approach.

2. Topological Data Structures for a 3D Finite Element Model

We shall restrict our attention to tetrahedral triangulations and regard the computational model as a three-dimension simplicial complex [20–22]. In addition, we focus on the case of quadratic interpolation and, hence, every tetrahedron in the triangulation gives rise to a ten-node tetrahedral finite-element (e.g. [16]). Extensions to higher-order elements are straightforward, but will not be pursued here. The local nodal numbering convention for the tetrahedral elements adopted here is shown in Fig. 1(a). Each tetrahedron is bounded by exactly four triangular faces (Fig. 1(b)) and six edges (Fig. 1(c)). The faces and the edges can be oriented consistently by an appropriate ordering of the nodes (Figs 1(b) and 3(c)). A face is bounded by exactly three edges. Each face is incident on exactly one tetrahedron, if the face is on the boundary of the body, or two tetrahedra, if the face is in the interior (Fig. 2). Edges are incident on rings of varying numbers of tetrahedra. Likewise, a variable number of faces may be adjacent to an edge.

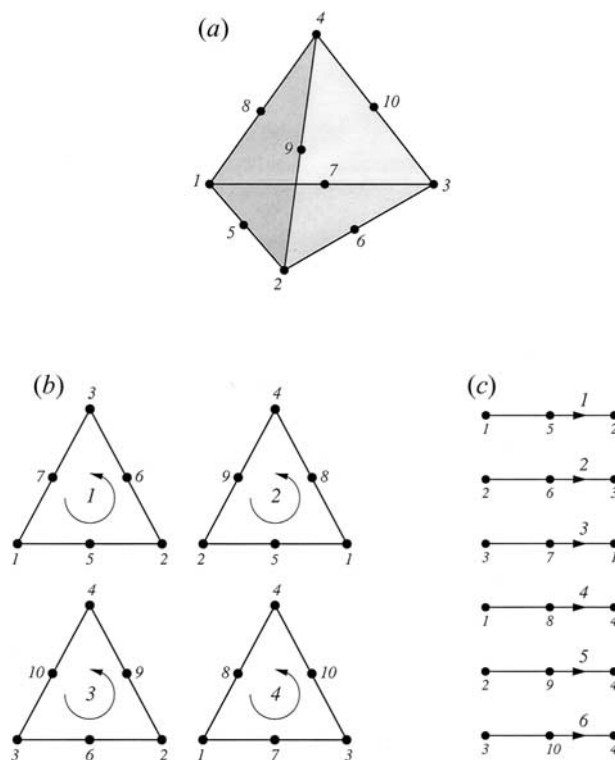


Fig. 1. (a) A 10-nodes tetrahedron (b) description of its four facets (c) description of its six segments.

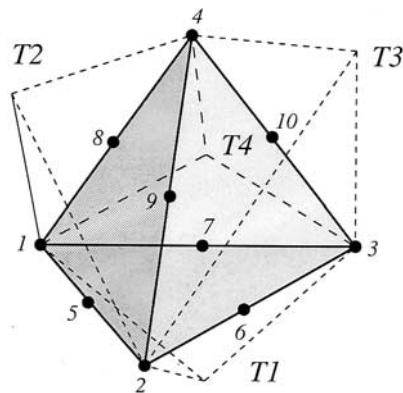


Fig. 2. Tetrahedron connected to four adjacent tetrahedra.

We begin by introducing three data structures which collect these data and relationships, namely, the tetrahedra, facets and segments structures. In describing these structures, we adopt C syntax for definiteness. The redundancy of data stored in our structures is justified by the need to speed up some additional searching procedure used in the mechanical applications.

The data stored in the tetrahedra structure consists of the number of the element, the element connectivity, pointers to its six segments, pointers

```

/*-----*
 * Tetrahedron data structure
 *-----*/
typedef struct tetra
{
    struct tetra *Link, *Rlink; /* Links */
    int el; /* Element no. */
    int N[10]; /* Nodes */
    struct segment *S[6]; /* Pointers to Segments */
    struct facet *F[4]; /* Pointers to Facets */
    struct tetra *T[4]; /* Pointers to Tets */
    int C[4]; /* Cohesive element */
    int L[4]; /* Coh. el. side: 0=bottom, 1=top */
} Tetra;

```

Fig. 3. Description of the tetrahedron data structure.

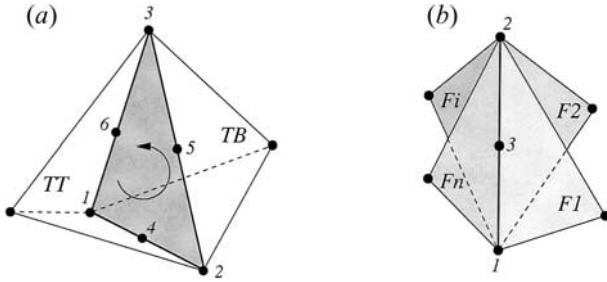


Fig. 4. (a) A facet connected to two tetrahedra; (b) a segment connected to several facets.

to its four facets and pointers to the four adjacent tetrahedra (Fig. 3). Some of these pointers can be null. For instance, if a tetrahedron is incident on the boundary one or more of the pointers to adjacent tetrahedra are null. With a view to facilitating fragmentation simulations based on the use of cohesive elements [12], we include in the tetrahedra structure the number of the adjacent cohesive elements and the side of the cohesive elements incident on the tetrahedron.

The data stored in the facet structure consists of an array containing six nodal numbers, ordered cyclically so as to define an orientation for the face; pointers to the top and bottom tetrahedra, defined in accordance with the orientation of the face (Fig. 4(a)); pointers to the three edges incident on the face; and a boolean variable indicative of whether the face is interior or exterior (Fig. 5). Specifically,

```

/*-----*
 * Facet data structure
 *-----*/
typedef struct facet
{
    struct facet *Link, *Rlink; /* Links */
    int N[6]; /* Nodes */
    struct tetra *T[2]; /* Pointers to Tets */
    struct segment *S[3]; /* Pointers to Segments */
    int posi; /* 0 = internal, 1 = external */
    double v[3]; /* Components of the unit normal */
    double sc; /* Traction limit value */
    int cm; /* Cohesive material index */
} Facet;

```

Fig. 5. Description of the facet data structure.

the identify top (bottom) or positive (negative) tetrahedron is that tetrahedron from which the nodes of the facet appear to be traversed counter-clockwise (clockwise). For facets which are on the surface, the bottom tetrahedron is null. With a view to fragmentation applications, we additionally collect the components of the unit normal; the critical traction for the insertion of a cohesive element, and an index designating the cohesive law to be used within the cohesive element.

The edge structure segment contains an array with the numbers of its three nodes (Fig. 6), all of which are shared with one or more adjacent facets and with one or more adjacent tetrahedra. The local sequential numbering of the nodes defines the orientation of the edge. Owing to the variable environment of the edges in the triangulation, the structure segments additionally contains arrays of pointers which need to be allocated dynamically. These are the array of pointers to the tetrahedra and faces adjacent to the edge. The dimension of these arrays is also stored in the structure, as well as an additional boolean variable which designates the edge as interior or exterior.

A C procedure for setting up the structures just described from a conventional finite-element connectivity array is shown in Appendix A.

3. Fragmentation

Ortiz and Pandolfi [23] developed a class of three-dimensional cohesive elements consisting of two six-node triangular facets (Fig. 7(a)). The opening displacements are described by quadratic interpolation within the element. The element is fully compatible with – and may be used to bridge – pairs of ten-node tetrahedral elements (Fig. 7(b)). The elements are endowed with full finite-deformation kinematics and, in particular, are exactly invariant with respect to superposed rigid body translations and rotations.

```

/*-----*
 * Segment data structure
 *-----*/
typedef struct segment
{
    struct segment *Link, *Rlink; /* Links */
    int N[3]; /* Nodes */
    int nt; /* No. adj tets */
    struct tetra **T; /* Pointers to the first Tet */
    int nf; /* No. adj Facets */
    struct facet **F; /* Pointer to the first Facet */
    int posi; /* 0 = internal, 1 = external */
} Segment;

```

Fig. 6. Description of the segment data structure.

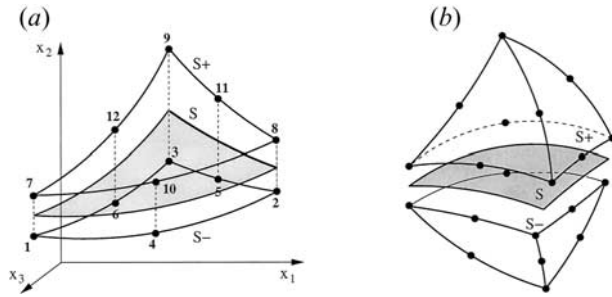


Fig. 7. (a) Geometry and connectivities of 12-nodes cohesive element; (b) assembly of 12-node triangular cohesive element and two 10-node tetrahedral elements.

We are here specially concerned with dynamic fragmentation, although static applications may be treated similarly. The analysis proceeds incrementally in time, e.g. by explicit dynamics. Following Camacho and Ortiz [5], cohesive elements are introduced adaptively at element interfaces as required by a fracture (or spall) criterion. For instance, fracture may be supposed to initiate at a previously coherent element interface when a suitably defined *effective traction* attains a critical value [5,24,23]. When the fracture criterion is met at an element interface, a cohesive element is inserted, leading to the creation of new surface. In this manner, the shape and location of successive crack fronts is itself an outcome of the calculations.

Next we discuss how the data structures defined in the preceding section may be used to support fragmentation simulations of the type just described. In particular, we specifically address the issue of how to update the data structures in response to fragmentation. The update procedure consists of two basic operations:

1. Selection of interior faces (*facets*) for the insertion of new cohesive elements.
2. Updating the data structures based on the selected *facets*.

We discuss these two steps in turn.

3.1. Selection of Faces to be Fractured

The selection of an interior face for the insertion of a cohesive element is based on the attainment of a suitable fracture criterion. The specific form of this criterion depends upon the type of cohesive model used in calculations. For definiteness, we consider the class of cohesive laws proposed elsewhere [5,24,23], which are based on the introduction of an effective opening displacement and the corresponding work-conjugate effective traction:

$$t_{eff} = \sqrt{t_n^2 + \beta^{-2} |\mathbf{t}_s|^2} \quad (1)$$

where β is a tension-shear coupling parameter, t_n denotes the traction component normal to the facet, and \mathbf{t}_s is the corresponding tangential traction (Fig. 8). If, in addition, cohesive surfaces are assumed to be rigid, or perfectly coherent, below a certain critical traction σ_c , or spall strength, then the appropriate form of the fracture criterion is

$$t_{eff} \geq \sigma_c \quad (2)$$

This condition is checked for each internal face (for example, at the integration points) at the conclusion of a prespecified number of time steps in the calculations, and the faces where the criterion is met are flagged for subsequent processing. Evidently, criterion (2), which arises directly from the mechanics of cohesive fracture, drives the evolution of the geometrical description of the model. This connection exemplifies the tight coupling between mechanics and geometry which is characteristic of fragmentation simulations.

3.2. Data-structure Update

The operations to perform in order to process a fractured face depend critically upon its position with respect to the external boundaries of the domain. Four main cases may be identified, depending upon whether the fractured facet has zero, one, two or three segments resting on the boundary (Fig. 9). This information is supplied by the flag *posi* of each segment contained in the facet. In all cases, the fractured facet is duplicated and a new facet is added to the corresponding linked list. The remaining operations to be performed are:

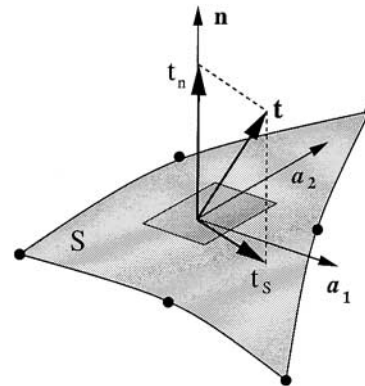


Fig. 8. Normal and tangential components of the traction acting on an interface.

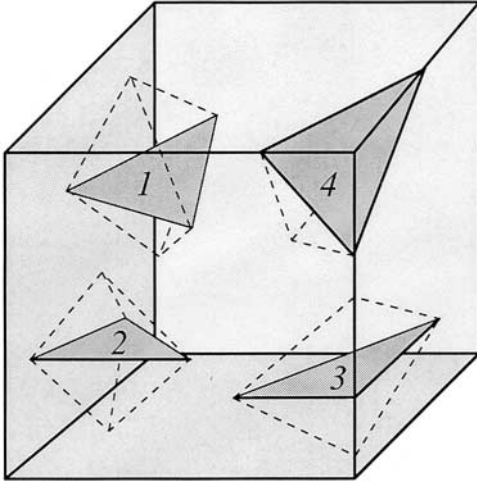


Fig. 9. Classification of cases according to whether the fractured facet has zero (case 1), one (case 2), two (case 3) or three (case 4) segments on the boundary.

1. No segments are on the boundary: No further operations (Fig. 10(a)).
2. One segment is on the boundary: the segment is duplicated by doubling the mid-side node (Fig. 10(b)).
3. Two segments are on the boundary: the segments are duplicated by doubling the mid-side nodes; the corner node is duplicated when it represents the sole remaining connection between the top and bottom tetrahedra (Fig. 10(c)).
4. Three segments are on the boundary: the segments are duplicated by doubling the mid-side nodes; a corner node is duplicated when it represents the sole remaining connection between the top and bottom tetrahedra (Fig. 10(d)).

The new nodes are added to the top elements of the fractured facet.

The commented C code reported in Appendix B gives a detailed account of the operations to be performed to update the data structures and the connectivities.

4. Examples of Application

In this section we demonstrate the scope and versatility of the procedures described above with the aid of two examples of application. The fracture criterion (2) is adopted to determine the onset of fracture in a facet [5,24,23]. In all calculations, the material is modeled as nonlinear elastic obeying a Neo-Hookean constitutive law [25]. In particular, full finite kinematics is taken into account.

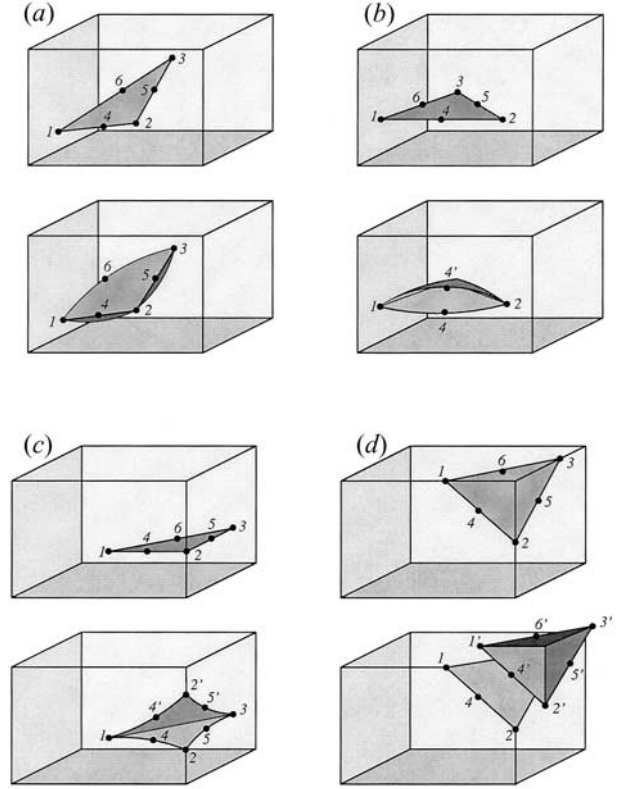


Fig. 10. Topological changes induced by the fracturing of a facet. The primed numbers indicate the new inserted nodes. (a) Case 1: no segments on the boundary. No action; (b) Case 2: one segment on the boundary. The mid-side node is duplicated; (c) Case 3: two segments on the boundary. The corner node is duplicated and the mid-side nodes are duplicated; (d) Case 4: three segments on the boundary. All six nodes are duplicated.

The first application concerns the simulation of the dynamic fragmentation of a three-point bend PMMA specimen with a sharp precrack contained within its symmetry plane. The central point of the top side of the specimen is suddenly imparted a uniform velocity 40 m/s at time $t = 0$, and the velocity is held constant thereafter. The length of the specimen is 8.4 mm, its width 1 mm and its height 1.4 mm (Fig. 11).

The model is meshed into 4260 ten-node tetrahedra and 6420 nodes. The mesh is finer in the central part and is gradually coarsened away from the crack (Fig. 12(a)).

The material parameters employed in the calculations are: specific fracture energy per unit area, or critical energy release rate, $G_c = 210$ N/m; critical cohesive stress, or spall strength, $\sigma_c = 100$ MPa; tension-coupling constant $\beta = 1$; Young's modulus $E = 3$ GPa; Poisson's ratio = 0.38; and mass density $\rho = 1180$ kg/m³. The equations of motion

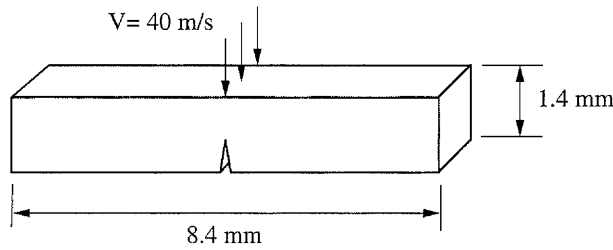


Fig. 11. Three point bend test in PMMA specimen, loading conditions. The impact is simulated imposing a uniform and constant velocity V along the central line. Owing to the high impact speed, the supports are not simulated.

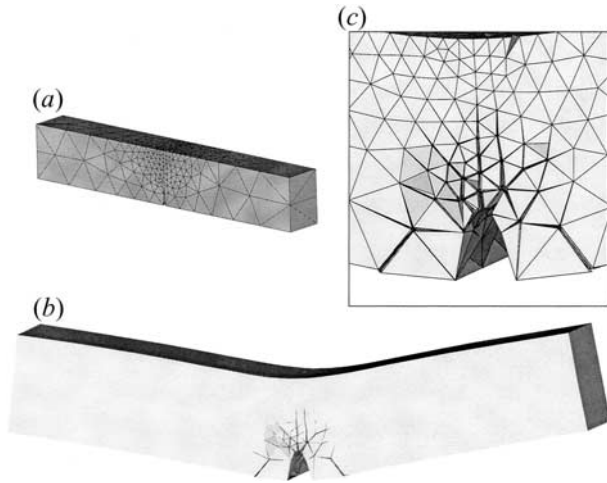


Fig. 12. Fragmentation algorithm applied to the three-point bend dynamic test in PMMA: (a) initial mesh; (b) final configuration; (c) detail of the fracture and fragmentation pattern in the final configuration.

are integrated in time by recourse to Newmark's explicit algorithm with parameters $\beta = 0$, $\gamma = 1/2$ [26,27]. The time step used in the calculations is $\Delta t = 1.7 \times 10^{-4} \mu s$.

Figures 12(b) and (c) show the computed fracture and fragmentation pattern after $20 \mu s$. The ability of the approach to track the evolution of complex crack geometries is clearly demonstrated. As may be seen in the figure, the geometrical update procedure effectively deals with the intricate geometrical and topological transitions which result from crack branching, the nucleation of surfaces and interior cracks, crack coalescence, the detachment of fragments, and others.

The second example of application concerns the simulation of dynamic crack branching in a PMMA thin square plate. The plate is 3 mm in length and 0.3 mm in thickness. The specimen contains an initial 0.25 mm sharp notch. Constant normal velo-

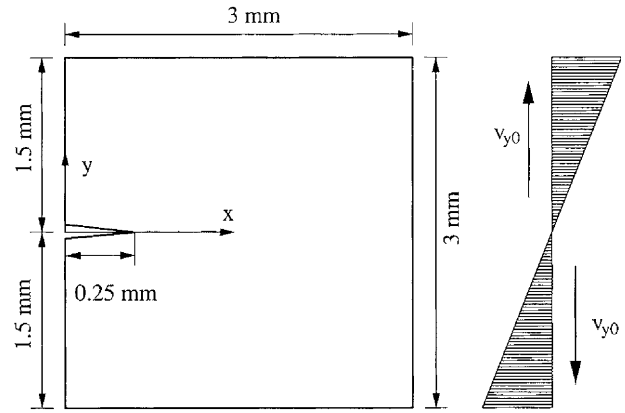


Fig. 13. Geometry of the PMMA square plate and mode-I loading conditions.

cities, tending to open the crack symmetrically in mode I, are prescribed on the top and bottom edges of the specimen. The magnitude of the prescribed velocities corresponds to a nominal strain rate of $0.002/\mu s$. In addition, the initial velocity field is assumed to be linear in the coordinate normal to the crack and to correspond to a uniform rate of deformation of $0.002/\mu s$ throughout the specimen (Fig. 13).

The model is meshed into 14,319 ten-node tetrahedra and 25,936 nodes (Fig. 14(a)). The equations of motion are integrated using Newmark's explicit algorithm with time step $\Delta t = 6 \times 10^{-5} \mu s$. The material parameters used in the calculation are: specific fracture energy per unit area $G_c = 176.15 \text{ N/m}$; critical cohesive stress $\sigma_c = 324 \text{ MPa}$;

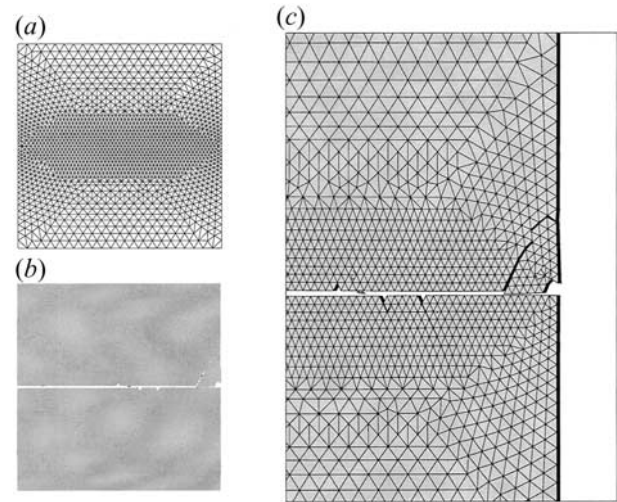


Fig. 14. Mode-I dynamic fracture test in PMMA at nominal strain rate $0.002/\mu s$. (a) Initial mesh and prescribed and initial velocities; (b) final configuration; (c) detail of the branching in the final configuration at time $5 \mu s$.

tension-shear coupling constant $\beta = 2$; Young's modulus $E = 3.29$ GPa; Poisson's ratio $= 0.35$; and mass density $\rho = 1190$ kg/m³. Figures 14(b) and (c) show the fracture pattern at the conclusion of the test. As may be seen, at a low prescribed strain rate the crack tends to grow within its plane, and it branches only when it senses the proximity of the free surface on the right side of the specimen. Results from a similar calculation at a higher nominal strain rate of $0.01/\mu\text{s}$ are shown in Figs. 15(a)–(c). The mesh in this case contains 6363 ten-node tetrahedra and 11,569 nodes, and the stable time step is $\Delta t = 6 \times 10^{-5} \mu\text{s}$. Figures 15(b) and (c) show the crack patterns at the conclusion of the test. Initially, the crack remains within its plane and accelerates steadily. As a certain crack speed is attained, the crack begins to issue lateral branches. These branches consume additional fracture energy, thereby limiting the mean crack speed. As the crack approaches the free surface, the extent of branching increases steadily.

As in the previous example, the ability of the method to deal with complex geometrical and topological transitions simply and effectively is remarkable. In particular, cracks are allowed to branch unimpeded, connect with free surfaces or with other cracks to form fragments.

We conclude this section by emphasizing that the simulations presented above, while representative of a broad class of engineering materials and loading conditions, are not intended as a validation of the cohesive model but as a demonstration of the com-

putational methodology. Detailed validation studies, including extensive comparisons with experiment, based on test configurations similar to those just described may be found elsewhere [7,8,9,28].

5. Summary and Conclusions

In cohesive theories of fracture, material separation is governed by a suitable cohesive law. In finite-element simulations based on a tetrahedral triangulation of the domain of analysis, decohesion and opening may conveniently be restricted to interior triangular faces. The cohesive laws considered here are rigid up to the attainment of the cohesive strength of the material. Consequently, initially all the faces in the triangulation are perfectly coherent, i.e. conforming in the usual finite element sense. Cohesive elements are inserted adaptively at interior faces when the effective traction acting on those face reaches the cohesive strength of the material. The insertion of cohesive elements changes the geometry of the boundary and, frequently, the topology of the model as well.

We have presented a simple set of data structures, and a collection of methods for constructing and updating the structures, designed to support the use of cohesive elements in simulations of fracture and fragmentation. The data structures and methods are straightforward to implement, and enable the efficient tracking of complex fracture and fragmentation processes. The examples of application discussed here illustrate the uncanny ability of the method to represent intricate geometrical and topological transitions resulting from crack branching, the nucleation of surfaces and interior cracks, crack coalescence, the detachment of fragments, and others.

Acknowledgements

The support of the Army Research Office through grant DAA-H04-96-1-0056 is gratefully acknowledged. We are also grateful for support provided by the DoE through Caltech's ASCI/ASAP Center for the Simulation of the Dynamic Behavior of Solids. The assistance provided by Dr. Rena Chengxiang Yu with the numerical examples is gratefully acknowledged.

References

1. Field, J.E., Sun, Q., Townsend, D. (1989) Ballistic impact of ceramics. Inst. Phys. Conf. Ser. No 102:

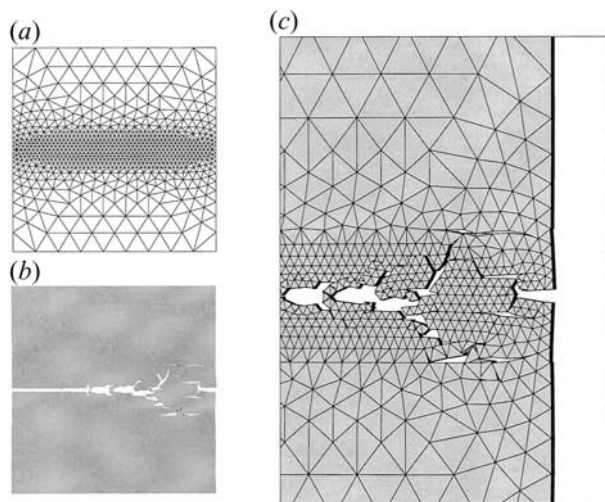


Fig. 15. Mode-I dynamic fracture test in PMMA at a nominal strain rate $0.01/\mu\text{s}$. (a) Initial mesh; (b) final configuration; (c) detail of the branching in the final configuration at time $5 \mu\text{s}$.

- Session 7, Int. Conf. Mech. Prop. Materials at High Rates of Strain, Oxford, UK
2. Kipp, M.E., Grady, D.E., Swegle, J.W. (1993) Numerical and experimental studies of high-velocity impact fragmentation. *Int. J. Impact Eng.* 14, 427–438
 3. Woodward, R.L., Gooch, W.A., O'Donnell, R.G., Perciballi, W.J., Baxter, B.J., Pattie, S.D. (1994) A study of fragmentation in the ballistic impact of ceramics. *Int. J. Impact Eng.* 15(5), 605–618
 4. Piekutowski, A.J. (1995) Fragmentation of a sphere initiated by hypervelocity impact with a thin sheet. *Int. J. Impact Eng.* 17, 627–638
 5. Camacho, G.T., Ortiz, M. (1996) Computational modelling of impact damage in brittle materials. *Int. J. Solids and Structures*. 33(20–22), 2899–2938
 6. Ortiz, M. (1996) Computational micromechanics. *Comput. Mech.* 18, 321–338
 7. Pandolfi, A., Krysl, P., Ortiz, M. (1990) Finite element simulation of ring expansion and fragmentation: The capturing of length and time scales through cohesive models of fracture. *Int. J. Fracture*, 95, 1–18
 8. Ruiz, G., Ortiz, M., Pandolfi, A. (2000) Three dimensional finite-element simulation of the dynamic brazilian tests on concrete cylinders. *Int. J. Numer. Meth. Eng.* 48(7), 963–994
 9. Ruiz, G., Pandolfi, A., Ortiz, M. (2001) Three-dimensional cohesive modeling of dynamic mixed-mode fracture. *Int. J. Numer. Meth. Eng.* 52(1–2), 97–120
 10. Ortiz, M., Suresh, S. (1993) Statistical properties of residual stresses and intergranular fracture in ceramic materials. *J. Appl. Mech.* 60, 77–84
 11. Xu, X.P., Needleman, A. (1994) Numerical simulations of fast crack growth in brittle solids. *J. Mech. Phys. Solids*, 42, 1397
 12. Pandolfi, A., Ortiz, M. (1998) Solid modeling aspects of three-dimensional fragmentation. *Eng. with Comput.* 14(4), 287–308
 13. Peraire, J., Vahdati, M., Morgan, K., Zienkiewicz, Q.C. (1987) Adaptive remeshing for compressible flow computations. *J. Comput. Phys.* 72, 449–466
 14. Peraire, J., Peiro, J., Formaggia, L., Morgan, K., Zienkiewicz, Q.C. (1988) Finite element euler computations in three dimensions. *Int. J. Numer. Meth. Eng.* 26, 2135–2159
 15. Löhner, R., Parikh, P. (1988) Generation of three-dimensional unstructure grids by the advancing-front method. *Int. J. Numer. Meth. Fluids*, 8, 1135–1149
 16. Radovitzky, R., Ortiz, M. (2000) Tetrahedral mesh generation based on node insertion in crystal lattice arrangements and advancing-front-Delaunay triangulation. *Comput. Meth. Appl. Mech. Eng.* 187(3–4), 543–569
 17. Kane, C., Repetto, E.A., Ortiz, M., Marsden, J.E. (1999) Finite element analysis of nonsmooth contact. *Comput. Meth. Appl. Mech. Eng.* 180, 1–26
 18. Molinari, J.F., Ortiz, M. (2002) Three-dimensional adaptive meshing by subdivision and edge-collapse in finite-deformation dynamic-plasticity problems with application to adiabatic shear banding. *Int. J. Numer. Meth. Eng.* 53(5), 1101–1126.
 19. Pandolfi, A., Kane, C., Ortiz, M., Marsden, J.E. (2002) Time-discretized variational formulation of nonsmooth frictional contact. *Int. J. Numer. Meth. Eng.* 53(8), 1801–1829
 20. Requicha, A.A.G. (1980) Representations for rigid solids: Theory, methods and systems. *Comput. Surv.* 12, 437–465
 21. Mantyla, M. (1988) *An Introduction to Solid Modeling*. Computer Science Press, Rockville, MD
 22. Hoffmann, C.M. (1989) *Geometric and Solid Modeling*. Morgan Kaufmann, San Mateo, CA
 23. Ortiz, M., Pandolfi, A. (1999) A class of cohesive elements for the simulation of three-dimensional crack propagation. *Int. J. Numer. Meth. Eng.* 44, 1267–1282
 24. De-Andrés A., Pérez, J.L., Ortiz, M. (1999) Elastoplastic finite element analysis of three-dimensional fatigue crack growth in aluminum shafts subjected to axial loading. *Int. J. Solids and Structures*, 36(15), 2231–2258
 25. Marsden, J.E., Hughes, T. (1983) *Mathematical Foundations of Elasticity*. Prentice Hall, Eaglewood CI: pps, NJ
 26. Belytschko, T. (1983) An overview of semidiscretization and time integration procedures. In: T. Belytschko, T.J.R. Hughes, eds, *Computational Methods for Transient Analysis*, North-Holland, Amsterdam, 1–65
 27. Hughes, T.J.R. (1983) Analysis of transient algorithms with particular reference to stability behavior. In: T. Belytschko, T.J.R. Hughes, eds, *Computational Methods for Transient Analysis*, North-Holland, Amsterdam, 67–135
 28. Yu, C., Pandolfi, A., Ortiz, M. (2002) 3d cohesive investigation on branching for brittle materials. In preparation

Appendix A

This procedure fills the data structures described in Figs 3–6. As the connectivity table is traversed, each element is added to the linked list of tetrahedra. The corresponding six segments of each tetrahedra are identified, and the linked list of the segments and the list of incident tetrahedra of the segments are updated. Likewise, the four facets of each tetrahedra are identified, and the linked list of the facets and the list of incident tetrahedra of the facets are updated. The subroutines are listed in the following boxes: (1) a new segment or facet insertion follows from the failure of a search in the corresponding linked lists; (2) the insertion of a new tetrahedron; (3) check of the existence of a segment in the corresponding linked lists; (4) the insertion of a new segment; (5) check of the existence of a facet in the corresponding linked lists; (6) the insertion of a new facet in the corresponding linked list; (7) update of the list of facet in the segment data structure.


```

int sc[6][4] = {{0,4,1},{1,5,2},{2,6,0}, /* segments topology */
               {0,7,3},{1,8,3},{2,9,3}};
int fc[4][6] = {{0,1,2,4,5,6},{0,3,1,7,8,4}, /* faces topology */
               {1,3,2,8,9,5},{0,2,3,6,9,7}};
int p1[3] = {1,2,0};
/*-----*/
* void CreateDataStructures
*-----*/
void CreateDataStructures ()
{
    Segment *S[6], *G;
    Facet *F[4], *R;
    Tetra *T, *Ti;
    int ie, ic, i, j, n[10];
    TetraList = NULL; /* Initialize the Tetrahedra list */
    SegmentList = NULL; /* Initialize the Segments list */
    FacetList = NULL; /* Initialize the Facets list */
    for (ie = 0; ie < TetraElementNumber; ie++) {
        /* Add Tetrahedron */
        for (j = 0; j < 10; j++) n[j] = connectivity[ie*nodes_element+j];
        TetraList = T = AddTetra (TetraList, n[0], n[1], n[2], n[3], n[4],
                                n[5], n[6], n[7], n[8], n[9], ie);
        for (ic = 0; ic < 6; ic++) { /* Add Segments */
            S[ic] = SearchInSegments (T, n[sc[ic][0]], n[sc[ic][1]],
                                    n[sc[ic][2]]);
            TetraList->S[ic] = S[ic];
        }
        for (ic = 0; ic < 4; ic++) { /* Add Facets */
            F[ic] = SearchInFacets (T, n[fc[ic][0]], n[fc[ic][1]],
                                   n[fc[ic][2]], n[fc[ic][3]],
                                   n[fc[ic][4]], n[fc[ic][5]]);
            for (j = 0; j < 3; j++) { /* Check Segments and Facets */
                for (i = 0; i < 6; i++)
                    if ((S[i]->N[0] == F[ic]->N[j] &&
                        S[i]->N[2] == F[ic]->N[p1[j]]) ||
                        (S[i]->N[2] == F[ic]->N[j] &&
                        S[i]->N[0] == F[ic]->N[p1[j]])) {
                        F[ic]->S[j] = S[i];
                        SegmentFacet (S[i], F[ic]);
                    }
            }
        }
        /* update the incident Facet */
        TetraList->F[ic] = F[ic];
    }
}

/* Complete the Tet list with adj Tets */
for (T = TetraList; T != NULL; T = T->Rink) {
    for (i = 0; i < 4; i++) {
        R = T->F[i];
        if (R->T[0] == T) T->T[i] = R->T[1];
        if (R->T[1] == T) T->T[i] = R->T[0];
    }
}

/* Complete the Facets list defining if inside or outside */
for (R = FacetList; R != NULL; R = R->Rink) {
    if (R->T[0] == NULL) R->posi = 1;
    if (R->T[1] == NULL) R->posi = 1;
}

/* Complete the Segment list defining if inside or outside */
for (G = SegmentList; G != NULL; G = G->Rink) {
    for (i = 0; i < G->nf; i++) {
        if (G->F[i]->posi == 1) G->posi = 1;
    }
}
return;
}

```

Appendix A.1

```

/*-----*/
* Tetra *AddTetra
*-----*/
Tetra *AddTetra (Tetra *beg, int n1, int n2, int n3, int n4, int n5,
                int n6, int n7, int n8, int n9, int n10, int ie)
{
    Tetra *T; /* Add a Tet to the linked list */
    T = calloc (1, sizeof(Tetra));
    T->el = ie + 1;
    T->N[0] = n1; T->N[1] = n2;
    T->N[2] = n3; T->N[3] = n4;
    T->N[4] = n5; T->N[5] = n6;
    T->N[6] = n7; T->N[7] = n8;
    T->N[8] = n9; T->N[9] = n10;
    T->C[0] = 0; T->C[1] = 0; T->C[2] = 0; T->C[3] = 0;
    T->Link = NULL;
    T->Rink = beg;
    if (beg != NULL) beg->Link = T;
    return T;
}

```

Appendix A.2

```

/*-----*/
* Segment *SearchInSegments
*-----*/
Segment *SearchInSegment (Tetra *T, int n1, int n2, int n3)
{
    Segment *S; /* Search for a Segment in SegmentList */
    int nt;
    for (S = SegmentList; S != NULL; S = S->Rink) {
        if ((n1 == S->N[0] && n3 == S->N[2]) ||
            (n1 == S->N[2] && n3 == S->N[0])) {
            nt = S->nt;
            nt++;
            S->T = realloc (S->T, nt * sizeof(Tetra *));
            S->T[nt - 1] = T;
            S->nt = nt;
            return S;
        }
    }
    SegmentList = S = AddSegment (SegmentList, n1, n2, n3, T);
    return S;
}

```

Appendix A.3

```

/*-----*/
* Segment *AddSegment
*-----*/
Segment *AddSegment (Segment *beg, int n1, int n2, int n3, Tetra *T)
{
    Segment *S; /* Add a Segment to the linked list */
    S = calloc (1, sizeof(Segment));
    S->posi = 0;
    S->N[0] = n1; S->N[1] = n2; S->N[2] = n3;
    S->nt = 1;
    S->T = calloc (1, sizeof(Tetra *));
    S->T[0] = T;
    S->nf = 0;
    S->F = calloc (1, sizeof(Facet *));
    S->Rink = beg;
    S->Link = NULL;
    if (beg != NULL) beg->Link = S;
    return S;
}

```

Appendix A.4

```

/*-----*
 * Segment *SearchInFacets                                     *
 *-----*/
Facet *SearchInFacets (Tetra *T, int n1, int n2, int n3,
                      int n4, int n5, int n6)
{
    Facet *F;          /* Search for a Facet in the FacetList */
    for (F = FacetList; F != NULL; F = F->Rink) {
        if ((n1 == F->N[0] || n1 == F->N[1] || n1 == F->N[2]) &&
            (n2 == F->N[0] || n2 == F->N[1] || n2 == F->N[2]) &&
            (n3 == F->N[0] || n3 == F->N[1] || n3 == F->N[2])) {
            F->T[1] = T;
            return F;
        }
    }
    FacetList = F = AddFacet (FacetList, n1, n2, n3, n4, n5, n6, T);
    return F;
}

```

Appendix A.5

```

/*-----*
 * Facet *AddFacet                                           *
 *-----*/
Facet *AddFacet (Facet *beg, int n1, int n2, int n3,
                int n4, int n5, int n6, Tetra *T)
{
    Facet *F;          /* Add a Facet to the linked list */
    F = calloc (1, sizeof(Facet));
    F->posi = 0;
    F->N[0] = n1; F->N[1] = n2; F->N[2] = n3;
    F->N[3] = n4; F->N[4] = n5; F->N[5] = n6;
    F->T[0] = T;
    F->Rink = beg;
    F->Link = NULL;
    if (beg != NULL) beg->Link = F;
    return F;
}

```

Appendix A.6

```

/*-----*
 * void *SegmentFacet                                       *
 *-----*/
void SegmentFacet (Segment *S, Facet *F)
{
    int nf = S->nf;
    int j;
    for (j = 0; j < nf; j++) if (S->F[j] == F) return;
    AddFaceToSegment (S, F);
    return;
}
/*-----*
 * void *AddFaceToSegment                                   *
 *-----*/
void AddFaceToSegment (Segment *S, Facet *F)
{
    int nf = S->nf;
    nf++;
    S->F = realloc (S->F, nf*sizeof(Facet));
    S->F[nf - 1] = F;
    S->nf = nf;
    return;
}

```

Appendix A.7

Appendix B

Code for the insertion of a new surface into a 3D mesh: (1) driver; (2) insertion of a new facet into the data structures; (3) changes in the data structures required by the duplication of a mid node; (Appendix A, 4) a new segment is added; (5) the list of the tetrahedra incident to the original segment is traversed and the tetrahedra are moved from the old to the new segment; (6) the list of the facets incident to the original segment is traversed and the facets are moved from the old to the new segment; (7) update of the cohesive element connectivity; (8) recursive subroutine to check the existence of additional connections between the Top and the Bottom tetrahedron before duplicating a corner node; (9) recursive subroutine to perform changes in the data structures required by the duplication of a corner node (the tetrahedron connectivity is update, and the incident segments and facets are updated; thus the adjacent tetrahedra are checked); (10) reallocation of the nodal vectors, (10) reallocation of element vectors. The last two subroutines must be completed with the reallocation of all the nodal and elemental vectors defined in the code.

```

/*-----*
 * void CreateSurface                                       *
 *-----*/
void CreateSurface (int cohmate, Facet *facet)
{
    Tetra   *TEB, *TET; /* Top and Bottom tetrahedra */
    int      open[3];   /* Boundary sides counters */
    Segment *S[3];      /* Facet Segments */
    Facet    *facetnew; /* New Facet */
    int      i, j;

    /* Get the six nodes on the Facet */
    for (i = 0; i < 6; i++) node[i] = nold[i] = facet->N[i];
    TET = facet->T[0];
    TEB = facet->T[1];
    for (i = 0; i < 3; i++) {
        S[i] = facet->S[i];
        open[i] = S[i]->posi;
    }
    /* add a new facet */
    FacetList = facetnew = AddFacet (FacetList, node[0], node[2], node[1],
                                     node[5], node[4], node[3], TET);
    UpdateNewFacet (facet, facetnew, TEB, TET, cohmate);
    for (i = 0; i < 3; i++) { /* Check the midside node */
        if (open[i] == 0) continue;
        nodes++;
        node[i + 3] = nodes;
        UpdateMidNodes (TET, S[i], node[i + 3], cohmate);
        DefineNodeVectors (node[i + 3], nold[i + 3]);
    }
    /* Check the corner node */
    counted = calloc (elements + 1, sizeof(int));
    for (i = 0; i < 3; i++) {
        if (open[i] == 0 || open[perm[i]] == 0) continue;
        for (j = 1; j <= TetraElementNumber; j++) counted[j] = 0;
        if (CornerToOpen (TET, TEB, nold[i]) == 0) continue;
        nodes++;
        node[i] = nodes;
        UpdateCornerNodes (TET, node[i], nold[i], cohmate);
        DefineNodeVectors (node[i], nold[i]);
    }
    free (counted);
    if (cohmate > 0) AddCohesive (cohmate, trli);
    return;
}

```

Appendix B.1

```

/*-----*
 * void UpdateNewFacet
 *-----*/
void UpdateNewFacet (Facet *facet, Facet *facetnew,
                    Tetra *TEB, Tetra *TET, int cohmate)
{
    Segment *S[3];
    int move[3] = {2,1,0};
    int i;
    /* Update the old Facet */
    facet->T[i] = NULL;
    facet->posi = 1;
    /* Update the new Facet */
    facetnew->posi = 1;
    /* Add Segments to new Facet and new Facet to Segments */
    for (i = 0; i < 3; i++) {
        S[i] = facet->S[i];
        S[i]->posi = 1;
        facetnew->S[move[i]] = S[i];
        S[i] = AddFaceToSegment (S[i], facetnew);
    }
    /* Update the Facet and adjacency of the Tets */
    for (i = 0; i < 4; i++) {
        if (TEB->F[i] == facet) {
            TEB->T[i] = NULL;
            if (cohmate > 0) {
                TEB->C[i] = elements + 1;
                TEB->L[i] = 0;
            }
        }
        if (TET->F[i] == facet) {
            TET->F[i] = facetnew;
            TET->T[i] = NULL;
            if (cohmate > 0) {
                TET->C[i] = elements + 1;
                TET->L[i] = 1;
            }
        }
    }
    return;
}

```

Appendix B.2

```

/*-----*
 * void UpdateMidNodes
 *-----*/
void UpdateMidNodes (Tetra *TET, Segment *S0, int nn, int cohmate)
{
    Segment *SN;
    Tetra *T;
    int n1 = S0->N[0];
    int n2 = S0->N[2];
    int ot = S0->nt;
    int of = S0->nf;

    /* Insert a new Segment */
    SegmentList = SN = AddSegment (SegmentList, n1, nn, n2, TET);
    SN->posi = 1;
    SN->nt = 0;

    /* Transfer Tets from the old to the new Segment */
    SN->T = realloc (SN->T, ot*sizeof(Tetra));
    TetraInSegments (TET, S0, SN, cohmate);
    SN->T = realloc (SN->T, SN->nt*sizeof(Tetra));
    S0->T = realloc (S0->T, S0->nt*sizeof(Tetra));

    /* Transfer Facets between the two Segments */
    SN->F = realloc (SN->F, of*sizeof(Facet));
    FacetInSegments (S0, SN);
    SN->F = realloc (SN->F, SN->nf*sizeof(Facet));
    S0->F = realloc (S0->F, S0->nf*sizeof(Facet));
    return;
}

```

Appendix B.3

```

/*-----*
 * void TetraInSegments
 *-----*/
void TetraInSegments (Tetra *TET, Segment *S0, Segment *SN, int cohmate)
{
    Tetra *T;
    int el = (TET->el - 1)*nodes_element;
    int no = S0->N[1];
    int nn = SN->N[1];
    int ot = S0->nt;
    int nt = SN->nt;
    int i, j;
    for (i = 4; i < 10; i++) { /* Change the connectivity */
        if (TET->N[i] != no) continue;
        TET->N[i] = connectivity[el + i] = nn;
        if (cohmate > 0) UpdateCohesive (TET, nn, no, 3);
    }
    for (j = 0; j < 6; j++) { /* Change the Segment in the Tet */
        if (TET->S[j] != S0) continue;
        TET->S[j] = SN;
    }
    for (i = 0; i < ot; i++) { /* Move Tet from old to new Segment */
        T = S0->T[i];
        if (T != TET) continue;
        SN->T[nt] = T;
        nt++;
        S0->T[i] = NULL;
        break;
    }
    SN->nt = nt;
    for (j = i + 1; j < ot; j++, i++) S0->T[i] = S0->T[j];
    ot--;
    S0->nt = ot;
    for (i = 0; i < ot; i++) { /* Look at adjacent Tets */
        T = S0->T[i];
        for (j = 0; j < 4; j++) {
            if (T->T[j] != TET) continue;
            TetraInSegments (T, S0, SN, cohmate);
            return;
        }
    }
    return;
}

```

Appendix B.4

```

/*-----*
 * void FacetInSegments
 *-----*/
void FacetInSegments (Segment *S0, Segment *SN)
{
    Tetra *T;
    Facet *F;
    int nn = SN->N[1];
    int of = 0;
    int nf = 0;
    int i, j, k;
    for (i = 0; i < SN->nt; i++) { /* Update connectivities */
        T = SN->T[i];
        for (j = 0; j < 4; j++) {
            F = T->F[j];
            for (k = 0; k < 3; k++) {
                if (F->S[k] != S0) continue;
                F->S[k] = SN;
                F->N[3 + k] = nn;
                SN->F[nf] = F;
                nf++;
                break;
            }
        }
    }
    SN->nf = nf;
    for (i = 0; i < S0->nt; i++) { /* Update the incident Facets */
        T = S0->T[i];
        for (j = 0; j < 4; j++) {
            F = T->F[j];
            for (k = 0; k < 3; k++) {
                if (F->S[k] != S0) continue;
                S0->F[of] = F;
                of++;
                break;
            }
        }
    }
    S0->nf = of;
    return;
}

```

Appendix B.5

```

/*-----*
 * void UpdateCohesive
 *-----*/
void UpdateCohesive (Tetra *T, int nn, int no, int add)
{
    int ce, cc, i, j;
    for (i = 0; i < 4; i++) {
        ce = T->C[i] - 1;
        if (ce < 0 || ce == elements) continue;
        cc = ce*nodes_element + T->L[i]*6 + add;
        for (j = 0; j < 3; j++) {
            if (connectivity[cc + j] != no) continue;
            connectivity[cc + j] = nn;
        }
    }
    return;
}

```

Appendix B.6

```

/*-----*
 * void CornerToOpen
 *-----*/
int CornerToOpen (Tetra *TET, Tetra *TEB, int no)
{
    Tetra *T;
    int i, j, res;
    counted [TET->el] = 1;
    for (i = 0; i < 4; i++) {
        T = TET->T[i];
        if (T == NULL) continue;
        for (j = 0; j < 4; j++) {
            if (T->N[j] != no) continue;
            if (T == TEB) return 0;
            if (counted[T->el] > 0) continue;
            if (CornerToOpen (T, TEB, no) == 0) return 0;
        }
    }
    return 1;
}

```

Appendix B.7

```

/*-----*
 * void UpdateCornerNodes
 *-----*/
void UpdateCornerNodes (Tetra *TET, int nn, int no, int cohmate)
{
    Segment *S;
    Facet *F;
    Tetra *T;
    int el = (TET->el - 1)*nodes_element;
    int j, i;

    counted[TET->el] = 0; /* Flag the Tet as checked */

    for (j = 0; j < 4; j++) { /* Check Tet and connectivity */
        if (TET->N[j] != no) continue;
        TET->N[j] = nn;
        connectivity[el + j] = nn;
        if (cohmate > 0) UpdateCohesive (TET, nn, no, 0);
        break;
    }

    for (j = 0; j < 6; j++) { /* Update Segments */
        S = TET->S[j];
        if (S->N[0] == no) S->N[0] = nn;
        if (S->N[2] == no) S->N[2] = nn;
    }

    for (i = 0; i < 4; i++) { /* Update Facets */
        F = TET->F[i];
        if (F->N[0] == no) F->N[0] = nn;
        if (F->N[1] == no) F->N[1] = nn;
        if (F->N[2] == no) F->N[2] = nn;
    }

    for (i = 0; i < 4; i++) { /* Next adjacency */
        T = TET->T[i];
        if (T == NULL) continue;
        if (counted[T->el] == 0) continue;
        UpdateCornerNodes (T, nn, no, cohmate);
    }
    return;
}

```

Appendix B.8

```

/*-----*
 * void DefineNodeVectors
 *-----*/
void DefineNodeVectors (int node, int nold)
{
    int nd = nodes*dof_node;
    int nn = (node - 1)*dof_node;
    int no = (nold - 1)*dof_node;
    int j;
    coordinates = realloc (coordinates, nd*REAL);
    for (j = 0; j < dof_node; j++) {
        coordinates[nn + j] = coordinates[no + j];
    }
    return;
}

```

Appendix B.9

```

/*-----*
 * void AddCohesive
 *-----*/
void AddCohesive (int cohmate, double trli)
{
    int k, i;
    k = nodes_element * elements;
    elements++;
    connectivity = realloc (connectivity, (k + 1)*sizeof(int));
    element_material = realloc (element_material, elements*sizeof(int));
    for (i = 0; i < 6; i++) {
        connectivity[k + i] = nold[i];
        connectivity[k + i + 6] = node[i];
    }
    element_material [elements - 1] = cohmate;
    return;
}

```

Appendix B.10